

FINITE ELEMENT ANALYSIS OF LARGE-SCALE REINFORCED CONCRETE SHELL OF DOMES

LAITH N. HUSSAIN, AHLAM S. MOHAMMED, AHMED A. MANSOR*

Ministry of Education, ThiQar's School Building Department, Iraq
*Corresponding Author: aamansor@engineering.uodiyala.edu.iq

Abstract

A shell structure can be defined as a solid continuum lying between two closely spaced curved surfaces. In this respect, it can be considered as the materialization of a curved surface. This study tries to improve the structural performance of the dome shell itself and also to select the best method to analyse the shell of domes with large diameters. Thus, the present study involves four methods to enhance shell structural behaviour. The first method is to reinforce shell with different percentages and locations of steel bars (in top and bottom fibre or both). The second method is to enhance shell structural performance by adding ribs beam. The third method is done by resting shell on ring beam, whereas, the last method is done by complaining ribs and ring beam together. The procedure includes secretion of spherical domes that have large diameters of 23.5 m with thickness dimension of 0.14 m. To analyse the four methods, four different finite element models have been done using ANSYS V.16.2. The study found out that reinforcing shells by steel bars with a varied type cent ages and different locations have the small influence to optimize shell performance as indicated by shear stress diagram and crack patent. On the other hand, rib beams contributed to deduct and translate meridian and hoop stresses away from rib beams only. There is a slight contribution to increase the maximum load Capacity of shells in both of the first and the second cases; otherwise there is a dramatic change in ultimate load capacity for domes which are resting on ring beam. Resting shell on the ring beam gives different behaviours for dome. The maximum value of deflection has been recorded on the top of this type of dome which was equal to 10.2 mm and the addition of two steel bar layers increase the maximum deflection to 14.6 mm. For all cases, there is no change in hoop stress value till a diameter of 8000 mm. When the diameter is more than 8000 mm, hoop stress values are increased for all cases except the shell which rested on shell (2RS-N, 2RS-B-N). Thus, there is no significant change in hoop stress value until a diameter of 12000 mm.

Keywords: ANSYS, Dome, Finite element method, Reinforced concrete, Spherical shell.

1. Introduction

Shells can be defined as the structures in which the thickness (width) is small compared to its two other alternative dimensions. Usually, a shell could geometrically be described by its thickness and the shape of its middle surface, which can be defined as the surface that passes midway between the top and bottom surface of the shell. Shells can be constructed with high thickness to the radius ratio. The behaviour of the shell is governed by the behaviour of its middle surface [1]. In recent years, many industrial branches have used thin shell structures to construct their structure applications such as roofs of industrial buildings, pressure vessels, space vehicles, nuclear reactors, and auditoriums [2, 3]. Nowadays, expansion of shell structures results in unpredicted possibilities and opportunity for the combined understanding of practical, functional, cost-effective and aesthetic aspects.

A good knowledge of the structural behaviour of shells is imperative for good shell design. It can vary hugely depending on kind of loads the shell is expected to carry. Shells are shape based structures where the shape influence the shells load carrying capacity. This structural geometry largely dictates the development of stresses in the shell elements. This has to keep in mind to avoid unwanted deformations and structural failure [4]. Numerous shell finite elements have been proposed but yet, there still several difficulties in analysing general shell structures. Moreover, it is difficult to identify which shell element is the most effective element type currently available, and to identify how to get more efficient shell analysis procedures.

In finite element modelling, an ideal element must be converged, not locked which contains no mechanisms. It is able to give accurate deflection results and to represent the actual behaviour for the structure. It is not to be based upon numerically adjusted factors and easy to be implemented in a computer [5].

Chen et al. [6] reported a lot of tests on conical concrete-shells; different properties of material were used. The results contained load-deformation reaction. Internal stresses and strain, as well as crack propagation patterns through the elastic, inelastic, and ultimate stress ranges were studied in his research.

An investigation was given by Manasrah [7] concerning the connection effectiveness for elements of the segmental cylindrical shell units subjected to knife-edge load at the crown. Eight full-scale shell unit models with four different distinct sorts of connections were building and tried. Every one of the proposed models was with 0.40 m width and 0.05m thickness. The leader of the crown was about 1 m and secured length was 4 m.

Ford [8] contemplated the stress-strain and fracture behaviour for both reinforced and un-reinforced concrete. This type of concrete was ranged from linear-elastic but brittle to tough and ductile by different mixes of rubbery methyl methacrylate. Such composite materials were observed to be an idyllic with the end goal of correlation with different material models accessible in the unmitigated NONSAP program.

Mississippi [9] announced the finding of a structural assessment of the 5 m diameter observatory dome structure developed by Observa-Dome facilities and laboratories.

A verification study based upon two independent methods A finite element solution and a newly developed analytical method for typical cylindrical shell roofs

were introduced by Ostovari-Dailamani [10]. These methods had been used to determine the spectra of natural vibration modes, displacements, stress resultants and accelerations of the shell under the action of the vertical motions of a selected earthquake. Also, these two methods indicate that inclusion of self-weight and additional superimposed loading can reduce the predicted natural frequencies.

The importance of the inclusion of in-plane modes for a cylindrical shell subject to the vertical component of a selected earthquake loading showed that these modes can have a major impact on the predicted levels of in-plane deformation and the associated membrane stresses. Therefore, depending on the type of earthquake should be included for reliable estimates of earthquake response. It is concluded that performing a modal analysis in which the effects of pre-loading are ignored could lead to serious underestimation of responses for large roof shells under earthquake loading.

Furthermore, a nonlinear snap buckling analysis showed that the snap buckling loads are much lower than the classical critical loads in cylindrical roof shell. The results also showed that the frequencies of a doubly curved shell are higher than a cylindrical shell. The increase in the natural frequencies resulted in much lower displacements and stress resultant responses in the doubly curved shell.

As to the literature review survey, it ought to be underscored that no investigation associated with the analysis of large concrete thin shell domes is established. So, this work can be considered as the first one in the field of the study of large thin shell concrete domes. This study also investigates the behaviour of the concrete shell using finite element method via ANSYS version 16.1 software. The shell performance is improved by four methods: reinforcement addition in meridian and hoop direction, enhancement the load carrying capacity of domes by rib beams running in the meridian direction, resting shell on ring beam and the last method is done by complaining ribs and ring beam together.

The assumed properties of concrete in this study were compressive strength $f'_c = 30$ MPa, modulus of elasticity $E_c = 24647$ MPa, and the steel properties were assumed yield strength $f_y = 595$ MPa, ultimate strength $f_u = 620$ MPa and modulus of elasticity $E_s = 200,000$ MPa.

2. Geometry and Boundary Conditions of Dome

The geometry of the analysed domes is shown in Fig. 1. The diameter of the domes is 23.5 m and the thickness is 0.14 m. Ribs, Ring beams details are explained as below. The dome is simply supported represented by providing roller support on the base area of shell, ribs and ring. The load was applied on the whole volutes of the shell of dome only. The details of the RC beam are represented in Fig. 1.

To generate maximum percent of the hoop and meridian stresses on the shell, roller support was selected and simulated in the base nodes of all simulated domes. In this regard, these nodes were constrained in UY only. The horizontal movement helped to identify the most affected area of the shell under vertical load and to evaluate the most important parameters that have direct influence on the structural behaviour of domes that should be considered in dome design approaches. All the adopted cases of domed were tested under the effect of self-weight and ultimate load capacity.

Ten models of domes have been developed to study all required parameters. Table 1 involves all types of simulated models by ANSYS version 16.1 software.

Figure 2 explains all the reinforcement details used in this study. Shell reinforcement was in meridian and hoop direction. Ring and ribs beam details were reinforced with high percentage of steel area to ensure that there is no fail happened on beam before shell. All details of steel reinforcement are listed in Table 2. The properties of the used material are illustrated in Table 3.

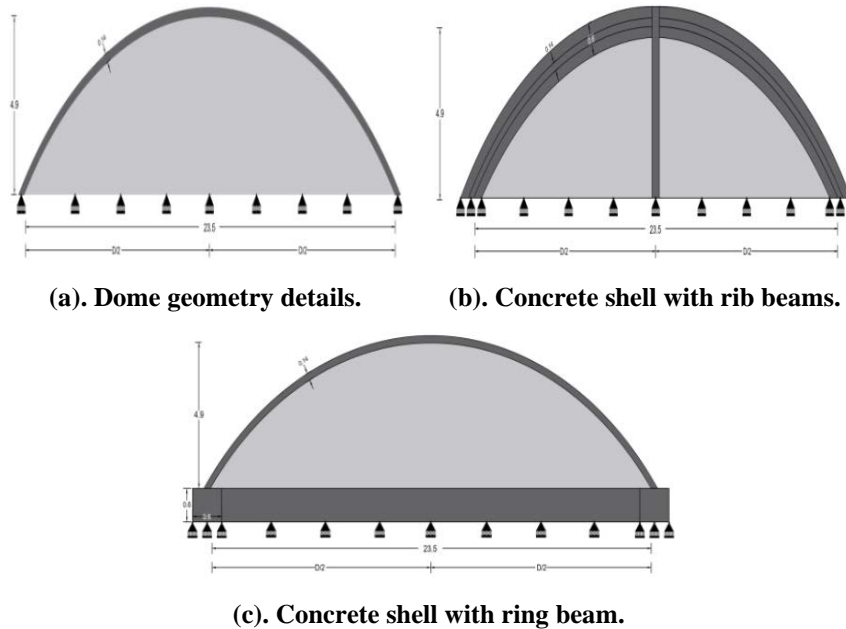
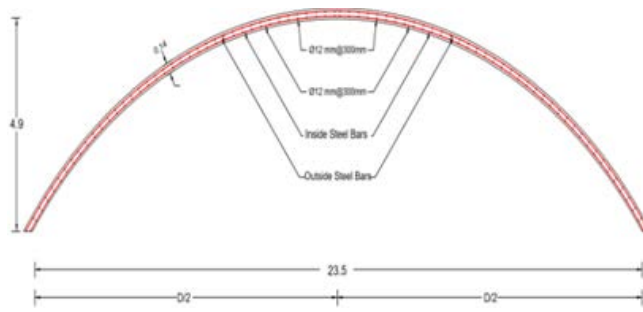


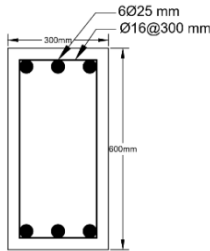
Fig. 1. Dome geometry details.

Table 1. Dome details.

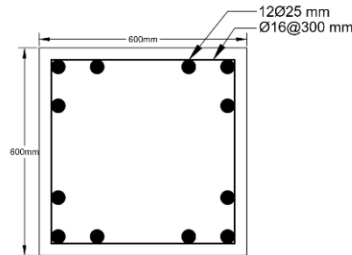
Cases and Dome Designation	Dome Elements		
	Number of Reinforcement Layers in Shell	Ring Size (mm)	Ribs Size (mm)
Case 1	S1	-	-
	RS-I	1	-
	RS-O	1	-
	RS-2	2	-
Case 2	RS-B	-	(300×600)
	2RS-B	2	(300×600)
Case 3	RS-N	(600×600)	-
	2RS-N	2	(600×600)
Case 4	RS-B-N	(600×600)	(300×600)
	2RS-B-N	2	(600×600)



(a). Shell reinforcement details.



(b). Rib beam details.



(c). Ring beam details.

Fig. 2. Shell, ribs and ring reinforcement details..

Table 2. Steel bar details of shell, ribs and ring beam.

Ribs	1	Longitudinal bars 6 ϕ 25mm
	2	Stirrups ϕ 16 @200 mm c/c
	3	Clear cover 40 mm
Ring	1	Longitudinal bars 12 ϕ 25mm
	2	Ties ϕ 20 @300 mmc/c
	3	Clear cover 40 mm
Shell	1	Meridional steel bars ϕ 12@300 mmc/c
	2	Hoop steel bars ϕ 12@ 300 mmc/c
	3	Cover 20 mm

Table 3. Material properties of typical dome.

For Concrete		value
E_c	Young modulus of elasticity, MPa	24647
f'_c	Compressive strength, MPa	30.0
γ	Poison's Ratio	0.2
density	kN/m ³	24
For Steel		
E_s	Young Modulus of elasticity (GPa)	200
f_y	Yielding stress, MPa	595
f_u	Ultimate stress, MPa	620
density	kN/m ³	77

3. Material Modeling

Reinforced concrete structures are made up mainly of two materials with different characteristics, namely, steel and concrete, the two materials are with very different physical and mechanical behaviours. Steel can be considered a homogeneous material. On the other hand, Concrete mechanical properties scatter cannot easily be defined. For the convenience of analysis and design, however, it is often considered as a homogeneous material in the macroscopic sense [11]. In the following, the behaviour of each constituent materials discussed separately.

3.1. Concrete modelling

The stress-strain relation of concrete is not only nonlinear but is different in tension than in compression. The mechanical properties of concrete are dependent on concrete age and on environmental conditions. The concrete is assumed to be an isotropic elastic material before cracking or crushing which is made due to the applied load. After crushing, the concrete is assumed to have lost its stiffness in all directions. After cracking, the concrete is assumed to be orthotropic having stiffness based on a bilinear softening stress-strain response in the crack normal direction.

In ANSYS, the stress-strain behaviour of the concrete can be defined by a piecewise linear stress-strain model in which the nonlinear stress-strain relation is approximated by a series of straight-line segments. Numerical expressions adopted by Desayi and Krishnan [12]. In the present work, Eq. (1) and (2) were used along with Eq. (3) adopted by Gere and Timoshenko [13] to construct the uniaxial compressive stress-strain (multilane anisotropic) curve for concrete.

$$f = \frac{E_c \varepsilon}{1 + \left(\frac{\varepsilon}{\varepsilon_0}\right)^2} \quad \varepsilon_1 \leq \varepsilon \leq \varepsilon_0 \quad (1)$$

$$\varepsilon_0 = \frac{2f'_c}{E_c} \quad (2)$$

$$f = \varepsilon E_c \quad 0 \leq \varepsilon \leq 0.3f'_c \quad (3)$$

$$f_c = f'_c \quad \varepsilon_0 \leq \varepsilon \leq \varepsilon_{cu}$$

$$\varepsilon_1 = \text{the strain corresponding to } 0.3f'_c = 0.3f'_c/E_c \quad (4)$$

where: f = stress at any strain ε (MPa), ε = strain at stress f , ε_0 = strain at the ultimate compressive strength f'_c .

Figure 3 shows the simplified compressive uniaxial stress-strain relationship that was used in this study. This curve is constructed from six points connected by straight lines. The curve starts at zero stress and strain. Point No. 1, at $0.3f'_c$, is calculated for the stress-strain relationship of the concrete in the linear range (Eq. 3). Point Nos. 2, 3, 4 and 5 are obtained from eq. (1), in which ε_0 is calculated from Eq. (2). Point No. 6 is at ε_0 and f'_c . In this study, an assumption was made of perfectly plastic behaviour after point No. 6.

3.2. Steel reinforcement modelling

The steel for the finite element models was assumed to be an elastic-perfectly plastic material and identical in tension and compression as could be shown in Fig. 4. This model required the modulus of elasticity of steel, Poisson's ratio of steel,

yield stress (f_y) to be input as a required information for ANSYS program. The stress-strain curve is assumed to be linearly elastic up to steel yield stress (f_y). As a result, the nonlinear plastic behaviour will start. The reason for this approximation is the computational convenience of the model. Perfect bond between the concrete and steel bars is assumed.

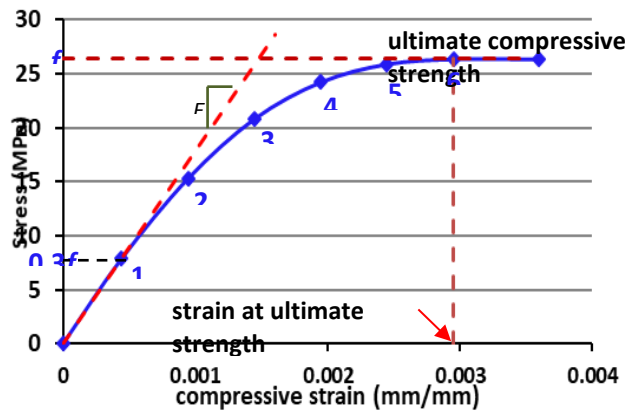


Fig. 3. Uniaxial stress-strain relationship for the concrete.

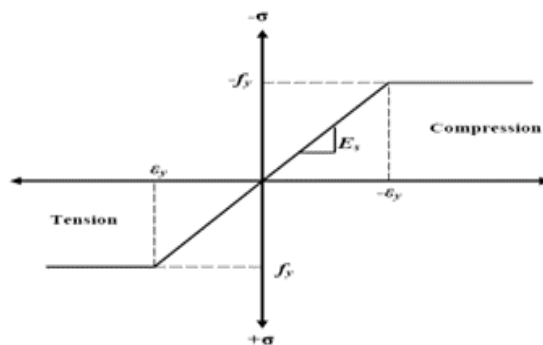


Fig. 4. Stress-strain curve for steel reinforcement [14].

4. Element Types

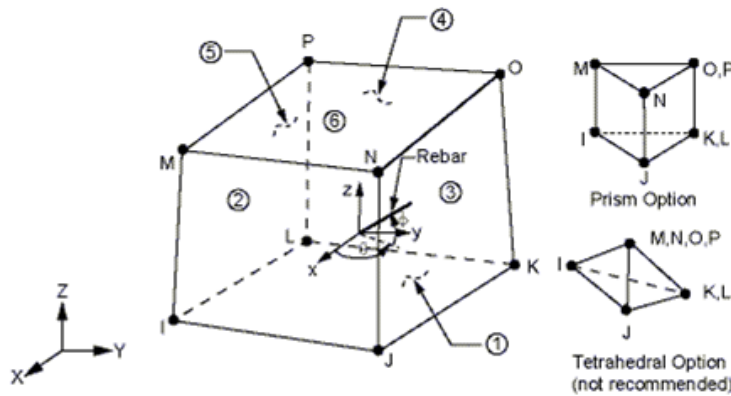
4.1. Elements used for concrete representation.

The present analysis included the influence of the concrete material conducted on the load capability and failure style of the construction. The type of component element utilized at this stage of the investigation is SOLID65 element for both shell and beams. SOLID65 is a solid element in the ANSYS library for 3D displaying of structures. The element is equipped for cracking in tension and crushing in compression. It is likewise equipped with plastic disfigurement and creep. Hence, it can demonstrate the model behaviour of the concrete material marked by a much lower strength in compression as well as in tension. The element incorporates a rebar capability that can model the behaviour of reinforcement concrete. The reinforcement could be characterized in three distinct directions. In the present study, the steel reinforcement is characterized to be smeared all through the

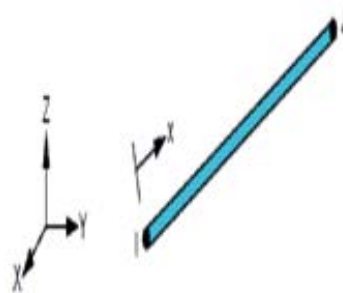
element. SOLID65 element has eight nodes with three DOFs per node (UX, UY and UZ). SOLID65 element is illustrated in Fig. 5(a).

4.2. Elements used for steel bars reinforcement

Beam188 element was utilized for modelling all steel bars. Discrete displaying is utilized by assuming that there is an ideal bonding between steel reinforcing bars and the concrete material. It is a quadratic beam element in 3-D. Link188 was designed to have two nodes with three DOFs per each node which were identical to solid65 nodes. Figure 5(b) illustrates this. These DOFs consist of translations in the x, y, and z directions and rotations about the x, y, and z directions.



(a). Solid 65 element.

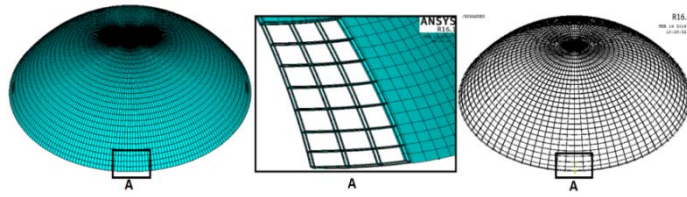


(b). Beam 188 element.

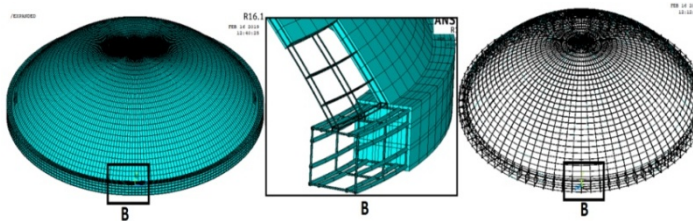
Fig. 5. Concrete and steel bar elements.

4.3. Assembly and meshing

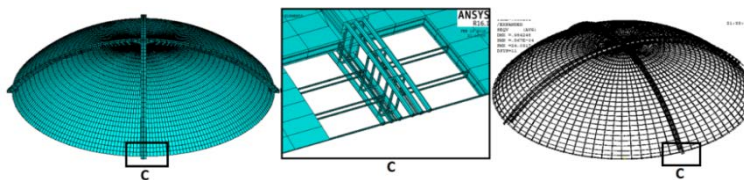
In order to get an accurate result, the sweeping rectangular element method was used for meshing volumes of all models. The finite elements illustration and the assembly for concrete and steel bars reinforcement in ANSYS model are shown in Fig. 6. In addition, all used elements are assigned the same mesh size to guarantee that every two different materials share the same node.



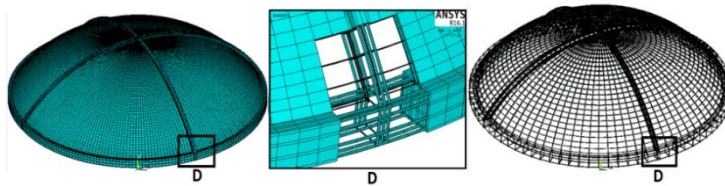
(a). Assembly elements of shell with steel bars.



(b). Assembly elements of shell and ring beam with steel bar element.



(c). Assembly elements of shell, ring and beam with steel bars.



(d). Assembly elements of shell and rib beams with steel bars.

Fig. 6. Assembly dome elements.

5. Results and Discussion

5.1. Deflection and ultimate load capacity results

Results including maximum deflections and ultimate loads capacity gained by strengthening technique in the present study are illustrated in Table 4. The bar chart in Figs. 7 and 8 show the deflections and ultimate load capacity for simulated model in this study. Load capacity slightly goes up in case one, which involved adding steel bar to shell in different percentages and different locations. Rib beam also contributed to increase the load capacity of reinforced and non-reinforced shell (RS-B and 2RS-B). The most dramatic change was caused in domes with ring beam. This value is closed to be increased four times in RS-N. Moreover, 2RS-N

in which shell contained two steel bar layer because that ultimate load capacity reaches to every large number. Finally, in the fourth case, the ultimate load capacity value continues increased by adding ribs beam.

Table 4. Deflections and ultimate load capacity.

Dome Designation	Max Deflection (mm)	Ultimate Load (kN)
Case 1	S1	0.135
	RS-I	1.069
	RS-O	1.071
	RS-2	1.077
Case 2	RS-B	0.962
	2RS-B	7.59
Case 3	RS-N	10.2
	2RS-N	14.66
Case 4	RS-B-N	7.06
	2RS-B-N	7.03

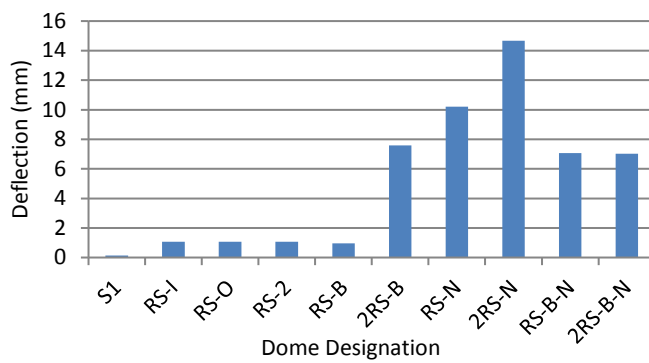


Fig. 7. Maximum deflection.

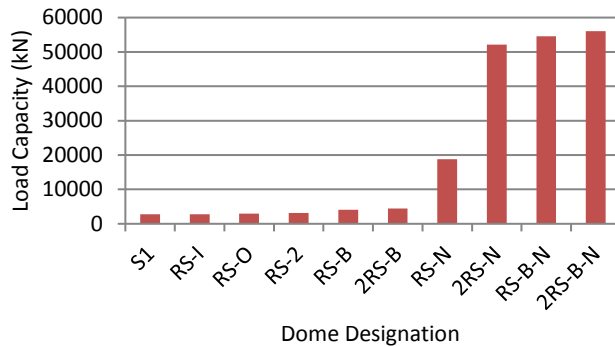


Fig. 8. Ultimate load capacity.

5.2. Dome deflected shapes

Resemble results for deflections were extracted from Fig. 9 for the first cases (S1, RS-I, RS-O and RS-2). The deflection values and their locations are almost the same. The maximum value was recorded at the top of shell and began to be reduced

gradually toward the bottom. Figure 10 illustrates the deflected shapes for case 2 .Adding rib beam has a significant change of dome performance. This beam enhances the nearby area of shell. The maximum deflection was recorded in the farthest area from ribs and adding two layers of steel bar contributed to deduct this area too much.

Resting shell on the ring beam gives different behaviours for the dome as can be seen in Fig. 11. The maximum value of deflection has been recorded on the top of this type of dome which was equal to 10.2 mm .The addition of two steel bar layers increases the maximum deflection to 14.6mm. Dome with ribs and ring beam have the same behaviour of the dome with ribs only, otherwise ring beam helps to move maximum deflection area toward top .The rib beam reduced steel bars effect on shells as illustrated in Fig. 12.

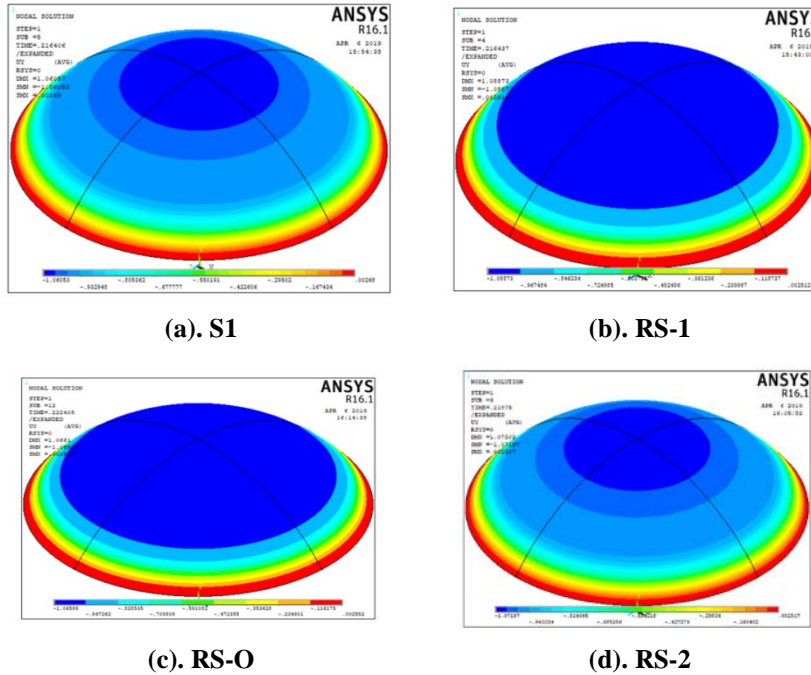


Fig. 9. Deflected shapes for Case 1.

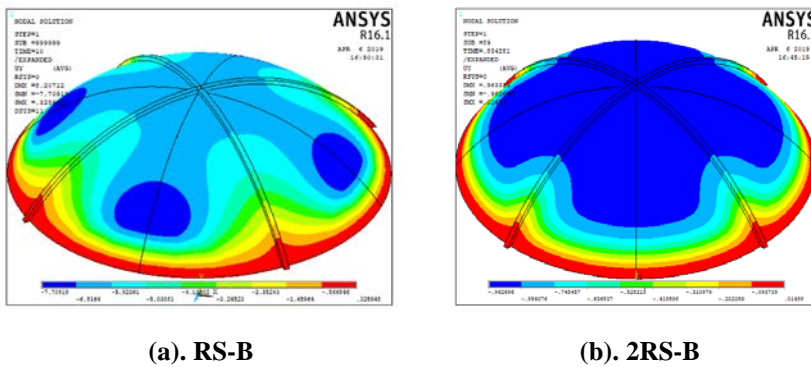


Fig. 10. Deflected shapes for Case 2.

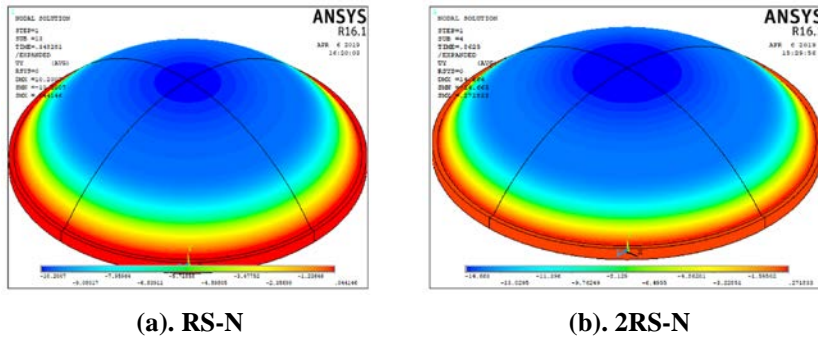


Fig. 11. Deflected shapes for Case 3.

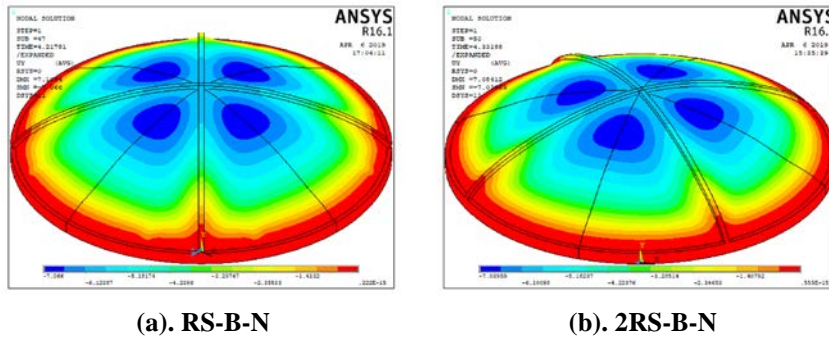


Fig. 12. Deflected shapes for Case 4.

5.3. Von Misses stress on domes

Von misses stress for whole discussed cases are shown in Figs. 13-16. This map of stresses distribution on domes under the ultimate load capacity helps to know and identify where the critical area is which were afford high stress. To improve dome performance, the designer should study this map carefully and should determine the most important parameters that have to be considered in dome design. Ribs and ring beam represent the main factor on distribution to obtained stress on dome shell. Whereas, the presence of steel bar layers in shell had slight effects as presented in Fig. 12. Table 5 illustrates the values of Von misses stress, knowing that the thickness of the dome was 140 mm.

Table 5. Von Misses stress/

Dome Designation	Von Misses Stress on Shell Steel Bars (MPa)	Von Misses Stress on Shell(MPa)
S1	-	5.33
Case 1	RS-I	22.42
	RS-O	18.05
	RS-2	5.4
Case 2	RS-B	5
	2RS-B	20
Case 3	RS-N	-
	2RS-N	485
Case 4	RS-B-N	-
	2RS-B-N	137

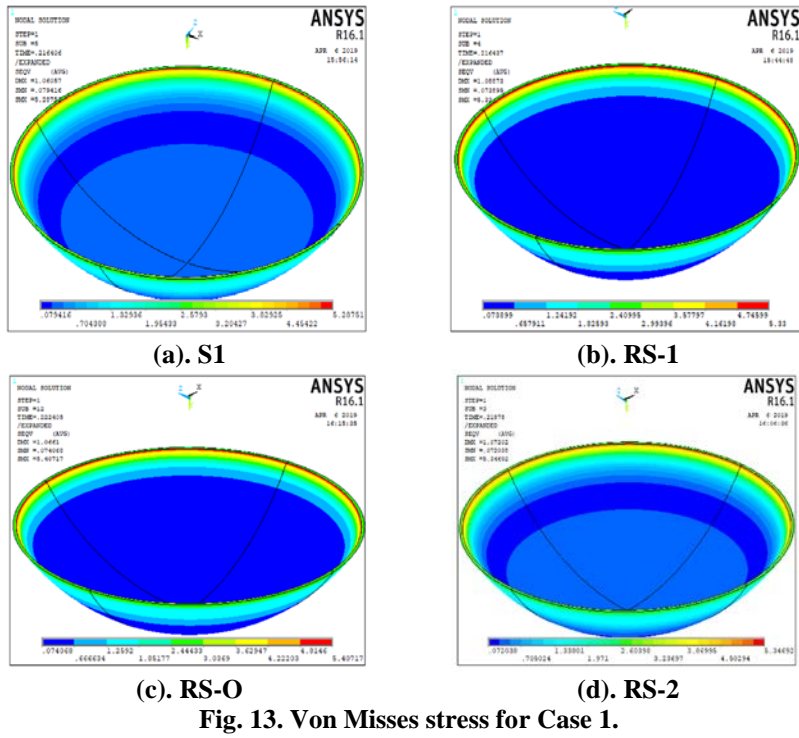


Fig. 13. Von Mises stress for Case 1.

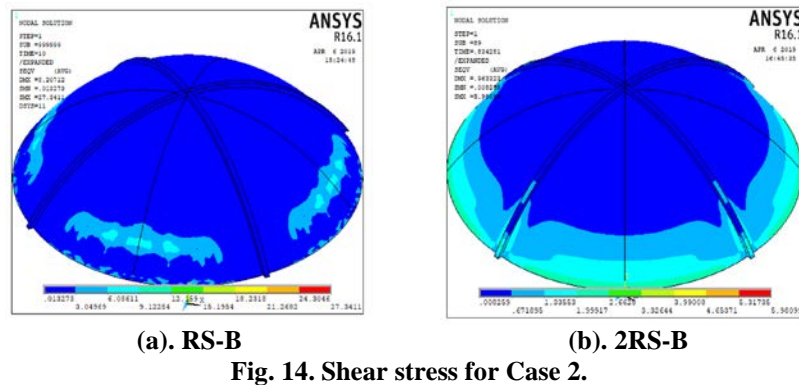


Fig. 14. Shear stress for Case 2.

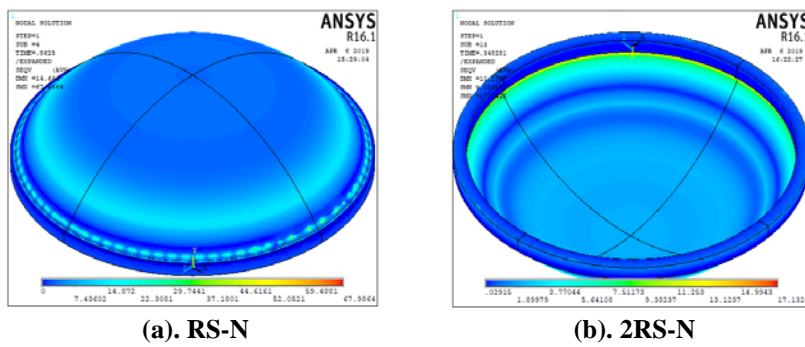


Fig. 15. Von Mises stress for Case 3.

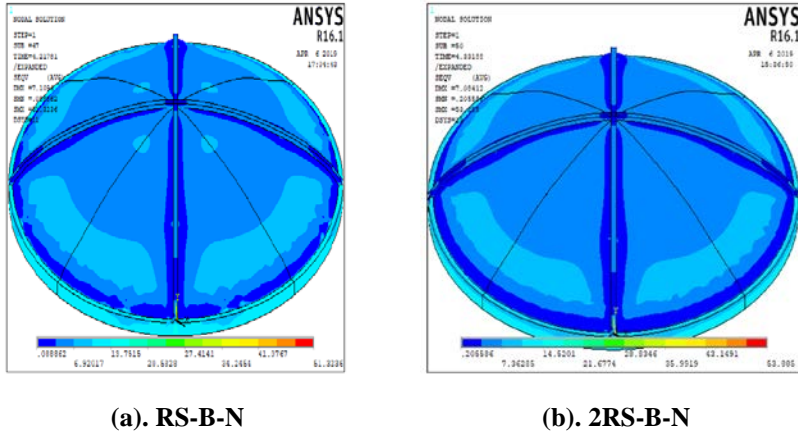


Fig. 16. Von Misses stress for Case 4.

5.4. Shear stress in hoop direction

The designer must identify the maximum value and locations of the generated stress in meridian and hoop direction. In this respect, this study selects the critical path of the generated hoop stresses in meridian direction of dome shell under self-weight as illustrated in Fig. 17.

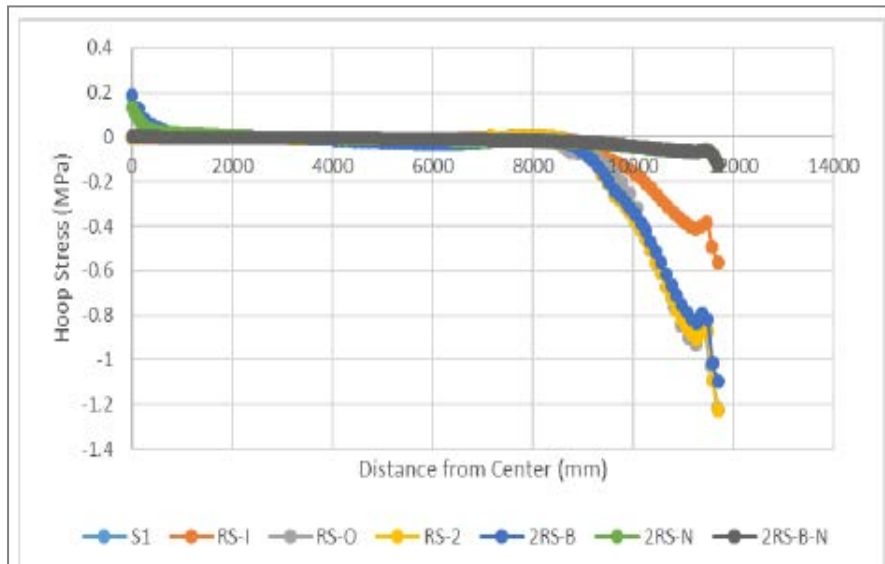


Fig. 17. Shell hoop stress on top fibre at self-weight load.

The ultimate load as illustrated in Fig. 18. To study the effect of the generated hoop stress on top fibre of shell for seven models, these models have been tested under a self-weight. The curve below provide good indicator to identify the maximum influenced area on shell. For all cases, there is no change in hoop stress value till diameter of 8000 mm. When the diameter is more than 8000 mm, hoop

stress values are increased for all cases except the shell which rested on shell (2RS-N, 2RS-B-N). There is no significant change in hoop stress value until a diameter of 12000 mm.

By selecting same baths on shells and applying the ultimate load (Fig. 16), the result helps to identify the actual behaviour of domes until the fail stage. The generated hoop stresses on shell top fibre creped to reach and cover most shell area. Hoop stress value creep is to cover shell from diameter 5000 mm for whole case while Hoop stress curve of 2RS,-N and 2RS-B-N stay homogeneous and soft with smallest value until shell base. So, the main important factor in dome performance was the existing of ring beam. Ring beam prevented hoop stress to move away from shell base toward other area. Steel reinforcement had no significant effect on redistribution of stress across shell while rib beam helped to expel stress from nearby places only.

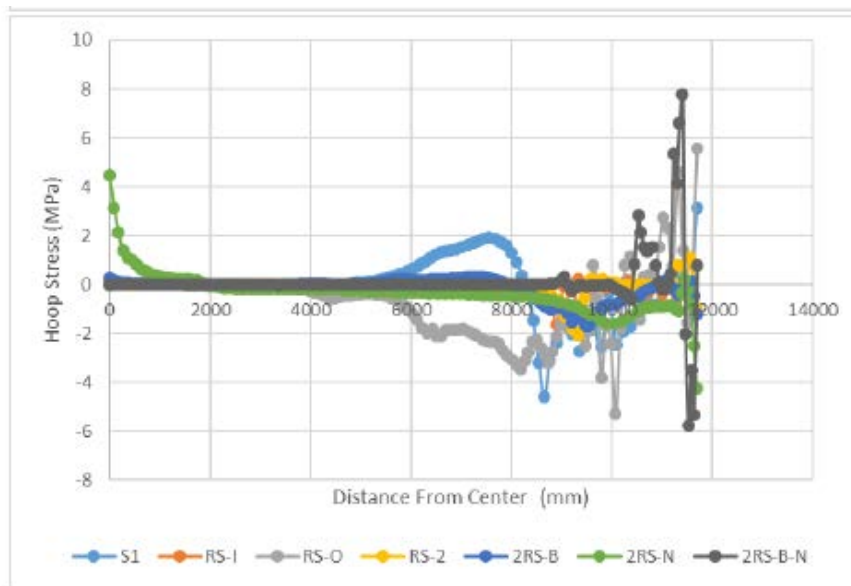


Fig. 18. Shell hoop stress on top fibre at ultimate load.

5.5. Crack patrons

Figure 19 illustrates the crack patrons appeared on quarter model of the domes under test. In general, cracks for all domes were separated in different places on shell. The simulated model helped to recognise the critical area on shell is and acknowledge the function of steel bar addition, rib addition and ring beams to dome. Steel bars with different percentages and different locations had no change on the location on shell. Rib beam function was to prevent crack to appear on closed area. Ring beam helped to enclose allowable area of crack to appear. This area was found just near base of shell.

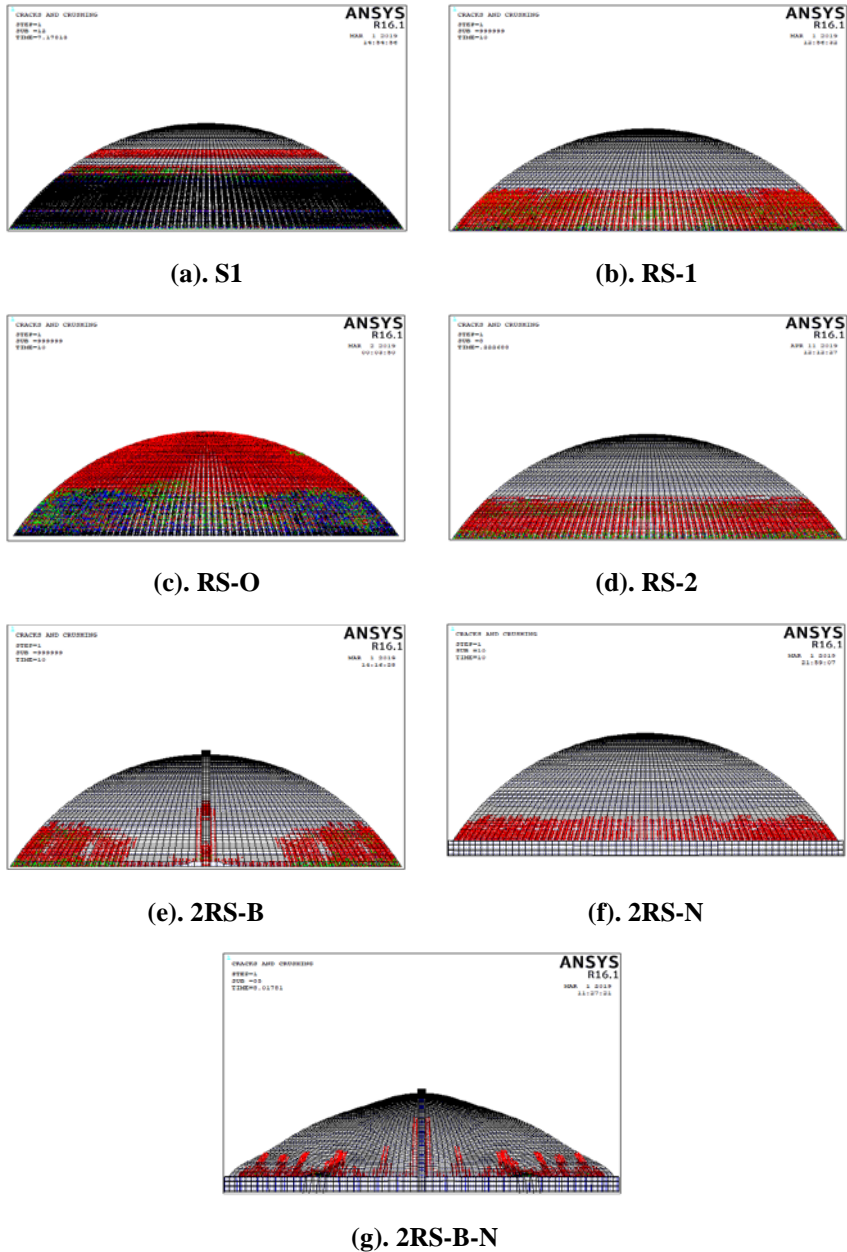


Fig. 19. Crack patrons.

6. Conclusions

An attempt to improve the performance of large diameter domes is introduced in the present work. As a result, the present research involved four methods to improve dome structural behaviour:

- First method was conducted by adding steel bars to shell in top and bottom fiber or bots (RS-I, RS-O and RS-2 respectively). The results of this method concluded that there is a slight contribution for the steel reinforcement in improving domes behaviour which was represented by increasing the ultimate load capacity and limiting and reducing the generated stresses. There are no benefits of adding steel bar more than the minimum percent of shrinkage.
- The second method was illustrated by adding rib beam running with shell. The study indicated that the rib beam has a good effect to improve shell performance just in closed area, so the fail was found on furthest area from rib beam. Rip beam has no big rule to optimize dome performance.
- Third method was represented by resting shell on ring beam which was the best method to take into consideration in improving the behaviour of domes with large diameter. The recorded load capacity was a very large number compared with the first and the second method. This capacity was almost three times when the shell contained steel bars.
- Lastly, in order to reach to the optimum performance of domes, ribs and ring beam have been complained. The extracted result shows that load capacity is slightly increased and the main function of rib beam in domes was to remove the generated stress from the closed area. Knowing the regions of stress consternation and the location of the minimum stress areas help in selecting the best zones for windows and other opening as an example.

Nomenclatures

E_c	Young modulus of elasticity for concrete, MPa
E_s	Young modulus of elasticity for steel, MPa
f'_c	Concrete compressive strength, MPa
f_u	Ultimate stress, MPa
f_y	Yielding stress, MPa

Greek Symbols

ϕ	Angle of Twist(rad.)
γ	Poison's Ratio

References

1. Bairagi, N.K. (1990). *Shell analysis*. (1st ed.). New Delhi: Khanna publishers.
2. Chandrashekhra, K. (1995). *Analysis of thin concrete shells*. (2nd ed.). Indian: New Age International Publishers.
3. Sun, G.; Longman, R.W.; Betti, R.; Che, Z.; and Xue, S. (2017). Observer Kalman filter identification of suspen-dome. *Mathematical Problems in Engineering*, 2Volume 2017, Article ID 1601534, 9 pages.
4. Kanta, N. (2015). *Design of thin concrete shell roof, for a basketball arena of 20,000 spectator capacity*. M.Sc. Thesis. Structural Engineering Department. Delft University of Technology.
5. Huang, H.C. (1989). *Static and dynamic analysis of plates and shells. theory. software and application*. New York: Springer-Valay, Berlin Heidelberg.

6. Chen, W.F.; Tse-Yung, P.C.; and Harshavardhan, C.M. (1979). Experiments on axially loaded concrete shells. *Journal of the Structural Division*, 105(8), 1673-1688.
7. Manasrah, A. (1993). *Ferrocement segmented shell structures*. M.Sc. Thesis. Civil Engineering Department, University of Technology, Baghdad, Iraq.
8. Ford, E. (1997). The theory and practice of impermanence. Article published in *Harvard Design Magazine*, No. 3, Harvard University Graduate School of Design, Harvard College.
9. Mississippi, J. (2002). The Finding of structural evaluation of the 5 meter diameter observatory dome structures. *Report of structural evaluation, Montgomery Hill Observatory*, Evergreen Valley College in San Jose, California, 1-52.
10. Ostovari-Dailamani, S. (2010). *Behavior of cylindrical and doubly-curved shell roofs under earthquake*. Ph.D dissertation. Department of Civil, Environmental and Geomatic Engineering .University College London.
11. Kwak, H.G.; and Filippou, C.F. (1990). Finite analysis concrete of reinforced concrete structures under monotonic loads. *A Report on Research Conducted under Grant*, RTA-59M848, Mechanics and Materials Department, Civil Engineering, University of California, Berkeley.
12. Desayi, P.; and Krishnan, S. (1964). Equation for the stress-strain curves of concrete. *ACI Journal*, 61(3), 345-350.
13. Gere, J.M.; and Timoshenko, S.P. (1997). *Mechanics of materials*. (4th ed.) PWS Publishing Company, Boston, Massachusetts.
14. Kachlakev, D.; Miller, T.; and Yim, S. (2001). Finite Element modeling of reinforced concrete structures strengthened with FRP laminates. *Final Report, Oregon Department of Transportation*, Research Group and Federal Highway Administration, Washington, DC 20590.s